Mon. Not. R. Astron. Soc. **000**, 1–?? (2002) Printed 19 November 2012 (MN LaTeX style file v2.2)

Assessment of Hill stability versus known chaos indicators: application to the dynamics of S-type extrasolar planets

S. Satyal,[1] B. Quarles,[1⋆] T.C. Hinse[2,3]
[1] *Department of Physics, University of Texas at Arlington, Arlington, Texas, 76019, USA.*
[2] *Korea Astronomy and Space Science Institute, 304-358 Daejeon, Republic of Korea.*
[3] *Armagh Observatory, College Hill, BT61 9DG, Armagh, UK.*

Released 2012 November 9

ABSTRACT

The efficacy of the Hill stability (HS) criterion is compared to other known chaos indicators such as the maximum Lyapunov exponent (MLE) and Mean Exponential Growth factor of Nearby Orbits (MEGNO) maps. The orbits of four individual planets in four known binary star systems, γ Cephei, Gliese 86, HD 41004, and HD 196885, are numerically integrated using various numerical techniques to assess the chaotic or quasi-periodic nature of the dynamical system considered. The Hill stability which measures the orbital perturbation of a planet around the primary star due to the secondary star is calculated for each system. The maximum Lyapunov exponent time series are generated to measure the divergence/convergence rate of stable manifolds, which are used to differentiate between chaotic and non-chaotic orbits. Then, we calculate dynamical MEGNO maps from solving the variational equations along with the equations of motion. These maps allow us to accurately differentiate between stable and unstable dynamical systems. The results obtained from the analysis of HS, MLE, and MEGNO maps are analysed for their dynamical variations and resemblance. The qualitative efficiency of each indicator is analysed which demonstrates that HS can be used as an alternative to MLE. The HS test for the planets shows stability and quasi-periodicity for at least ten million years. The MLE and the MEGNO maps have also indicated the local quasi-periodicity and global stability in relatively short integration period. Based on our discussion, the HS criterion is found to be a comparably efficient tool to measure the stability of planetary orbits with respect to different simulation timespans.

Key words: methods: numerical – methods: N-body simulations – celestial mechanics – binaries: general – stars: planetary systems

1 INTRODUCTION

The discovery of extra solar planets has been growing substantially since the first planet, 51 Pegasi b, was detected almost two decades ago (Mayor & Queloz 1995). Since then 843 extra solar planets have been confirmed as of October 22, 2012[1]. Near half of solar type stars (Duquennoy & Mayor 1991; Raghavan et al. 2006) and a third of all stars in the Galaxy (Raghavan et al. 2010) are in binary or multi-star system with 40 planets confirmed in such systems (Desidera & Barbieri 2007). The confirmation of the existence of planets in binaries has raised a new astrophysical challenge which includes the study of long term orbital stability of such planets. The ultimate destiny of exoplanet research, including observations from the Kepler mission[2], is to detect a planet on a stable orbit within the habitable zone of the host star (Borucki et al. 1997; Koch et al. 2007; Borucki et al. 2008, 2010). The degree of stability is largely governed by the planet's semi-major axis, eccentricity and orbital inclination. Orbital long-term stability is believed to be a necessary condition for life to develop. Our aim is to find an answer to the century old question, "Are we alone in the Milky Way Galaxy?".

By using different stability criteria the question of stability has been addressed by many others in the past. While studying the Trojan type orbits around Neptune, Zhou et al. (2009) showed that the inclination of orbits can be as high as 60^o while maintaining orbital stability. Several authors (Szebehely 1980; Szebehely & McKenzie 1981; Szenkovits

⋆ e-mail: billyq@uta.edu

[1] `www.exoplanet.eu`

[2] `www.nasa.gov/mission_pages/kepler/overview/index.html`

& Makó 2008) calculated orbital stability of planets by using several techniques that include the integrals of motion, zero velocity surfaces (ZVS), and a Hill stable region that is mapped by a parameter space of orbital radius and mass ratio, μ, for a coplanar circular restricted three body problem (CRTBP). Quarles et al. (2011) has also used the maximum Lyapunov exponent (MLE) to determine the orbital stability or instability for the CRTBP case. The stability limits were defined based on the values of MLE that are dependent on the mass ratio μ of the binaries and the initial distance ratio ρ_0 of the planet. Other chaos indicator techniques such as Mean Exponential Growth factor of Nearby Orbits (MEGNO) maps have also been used to study the dynamical stability of irregular satellites (Hinse et al. 2010) and extrasolar planet dynamics (Goździewski & Maciejewski 2001; Goździewski et al. 2001). The MEGNO criterion is known to be efficient in distinguishing between chaotic and quasi-periodic initial conditions within a dynamical phase space.

Knowing the orbital stability of planets is a crucial step for further studies of planetary systems. In order to probe a planet for its habitability, there exists a primary requirement that the system be orbitally stable. In this paper, we have used three well known chaos indicators HS, MLE, and MEGNO maps in the study of the orbital perturbation of planets in the selected stellar binaries. We have compared all the results from three different methods. The comparison study allows us to determine the best tool for a stability analysis of the considered systems.

This paper is outlined as follows. In Section 2 we discuss the basic theory of the analysis tools. In Section 3 we present our numerical methods and the results from the comparison of chaos indicators followed by discussion. Finally, we will conclude in Section 4 with a brief overview of our results.

2 THEORY

2.1 Basic Definitions and Equations

For the motion of a planet of mass m_1 around a star of mass m_2 in an orbital plane, the initial position of the planet at any given time is given by (Murray & Dermott 1999)

$$\begin{pmatrix} X \\ Y \\ Z \end{pmatrix} = r \begin{pmatrix} \cos\Omega\cos(\omega+f) - \sin\Omega\cos i\sin(\omega+f) \\ \sin\Omega\cos(\omega+f) + \cos\Omega\cos i\sin(\omega+f) \\ \sin i\sin(\omega+f) \end{pmatrix}, \tag{1}$$

where the orbital parameters (r, i, ω, Ω, f) are the radius vector, inclination angle, argument of periapsis, longitude of ascending node and true anomaly, respectively.

Then we can calculate the velocities in the x, y and z directions by taking the time derivative of Eq.(1) and obtain

$$\begin{aligned} V_x &= A\{e\sin f\,[\cos\Omega\cos(\omega+f) - \sin\Omega\cos i\sin(\omega+f)] \\ &\quad -(1+e\cos f)\,[\cos\Omega\sin(\omega+f) + \sin\Omega\cos i\cos(\omega+f)]\}, \\ V_y &= A\{e\sin f\,[\sin\Omega\cos(\omega+f) + \cos\Omega\cos i\sin(\omega+f)] \\ &\quad +(1+e\cos f)\,[\cos\Omega\cos i\cos(\omega+f) - \sin\Omega\sin(\omega+f)]\}, \\ V_z &= A\sin i\,[\cos(\omega+f)(1+e\cos f) + \sin(\Omega+f)e\sin f]. \end{aligned} \tag{2}$$

Equations (2) have been simplified using the following relations

$$\begin{aligned} \dot{f} &= \frac{na}{r\sqrt{1-e^2}}\,(1+e\cos f), \\ A &= \frac{na}{\sqrt{1-e^2}}, \end{aligned} \tag{3}$$

where ($\dot{f}$, n) are the time derivative of true anomaly and mean motion respectively. For our special case we considered the inclination $i = 0$ and while calculating the initial conditions we used the values of other parameters (Ω, ω and f) whenever they have been observationally determined.

Our particular interest is on the stellar binaries that are less than or equal to 25 AU apart. For the stars with greater than 25 AU separations, the effects of the secondary star on the planet would not be significant, especially while considering the intent of our present study.

The list of planets in the binaries and their orbital parameters are given in Tables 1 through 4. The initial setup in our simulations is in a barycentric coordinate system with Star B to the left and Star A to the right. The positive x-axis is taken to be the reference. The true anomaly and Right Ascension of ascending node of both the binary and planet are assumed to be equal to zero.

For two primaries in elliptic orbits moving about their barycentre the dynamical system of a third smaller mass can be written as the first order differential equations. The equations of motion are given below (Szebehely 1967; Szenkovits & Makó 2008)

$$\begin{aligned} x = \dot{u} \quad & u = 2v + \frac{1}{(1+e\cos f)}\left[x - \frac{\alpha(x+\mu)}{r_1^3} - \frac{\mu(x-1+\mu)}{r_2^3}\right], \\ y = \dot{v} \quad & v = -2u + \frac{y}{(1+e\cos f)}\left[1 - \frac{\alpha}{r_1^3} - \frac{\mu}{r_2^3}\right], \\ z = \dot{w} \quad & w = -z + \frac{z}{(1+e\cos f)}\left[1 - \frac{\alpha}{r_1^3} - \frac{\mu}{r_2^3}\right], \end{aligned} \tag{4}$$

where

$$\begin{aligned} \mu &= \frac{m_2}{(m_1+m_2)}, \\ \alpha &= 1-\mu, \\ r_1^2 &= (x-\mu)^2 + y^2 + z^2, \\ r_2^2 &= (x+\alpha)^2 + y^2 + z^2. \end{aligned} \tag{5}$$

The Jacobi constant (C_0) for a initial conditions (x_o, y_o, z_o, f_o) is given by

$$C_0 = \frac{x_0^2 + y_0^2 + \frac{2(1-\mu)}{r_1} + \frac{2\mu}{r_2}}{1+e\cos(f_0)} - \dot{x}_0^2 - \dot{y}_0^2 - \dot{z}_0^2. \tag{6}$$

In equations 4, the variables represent the velocity of a test particle (planet) in Cartesian coordinates (x, y, z). The distances r_1 and r_2 are defined in terms of mass ratio, normalised coordinates, and the position of the stars within a rotating coordinate system.

2.2 Lyapunov Exponents

For stable planetary orbits, the two nearby trajectories in phase space will converge and for unstable orbits, the

trajectories diverge exponentially. The rate of divergence is measured by using the method of Lyapunov exponents (Lyapunov 1907). Wolf et al. (1985) developed a numerical method of computing the Lyapunov exponents in FORTRAN following the earlier works by Benettin et al. (1980).

Lyapunov exponents are commonly used because they give the measure of an attractor of a dynamical system as it converges or diverges in phase space. The positive Lyapunov exponents measure the rate of divergence of neighboring orbits, whereas negative exponents measure the convergence rates between stable manifolds (Tsonis 1992; Ott 1993). The sum of all Lyapunov exponents is less than zero for dissipative systems (Musielak & Musielak 2009) and zero for non-dissipative (Hamiltonian) systems (Hilborn & Sprott 1994). Lyapunov exponents for the circular restricted three body problems (CRTBP) have been calculated previously (Gonczi & Froeschle 1981; Murray & Holman 2001). In this work, we have calculated the Lyapunov exponents for the elliptic restricted three body problem (ERTBP) and one case of the elliptic restricted four body problem (HD 41004). In order to calculate the Lyapunov exponents a dynamical system with n degrees of freedom is represented in a $2n$ phase space. Then for the case of ERTBP, state vectors ($2n$) containing 6 elements are used to calculate the Lyapunov exponents. The details on the calculation of Jacobian J from the equations of motion can be found in Quarles et al. (2011).

For a Hamiltonian system (see above) to be stable, the sum of all the Lyapunov exponents should be zero. In order to numerically meet such a criterion, a simulation of the system would require an impractically long period of time. Within the limits of simulation, the sum of all six exponents must remain numerically close ($\sim\ 10^{-10}$) to zero. We have used the largest positive Lyapunov exponent to determine the magnitude of the chaos while ignoring the lesser positive and the negative exponents as they do not provide significant additional information about the evolving system. The positive maximum Lyapunov exponent is known to indicate a chaotic behaviour in both dissipative (Hilborn & Sprott 1994) and non-dissipative (Ozorio de Almeida 1990) systems. Chaos can be proven up to the integration time if a given chaos indicator has converged to an unstable manifold. However, quasi-periodicity or regular motion can only be proven up to the considered integration time. Quasi-periodicity or stable motion can never rigorously be prooven for the 3 (or more) body system. We never know how the system might evolve after the considered integration time.

2.3 Hill Stability

Hill (1878a,b) developed the equations of motion for a particle around the primary mass in presence of a nearby secondary mass. The purpose of the Hill equations was to calculate the orbital perturbation of the particle due to the secondary mass. Later the idea was further developed and used in the study of orbital stability of planets (Szebehely 1967; Walker & Roy 1981; Marchal & Bozis 1982).

The significant radial gravitational influence of the secondary mass reaches as far as the Lagrange points, L1 and L2, forming the Hill sphere (Hill 1878a,b). The contour lines within the sphere are the zero velocity curves. After measuring a particle's position and velocity a constant of motion relation can be implemented (Szebehely 1967; Murray & Dermott 1999) $2U$ - $v^2 = C_J$, where v is the velocity, U is the generalised potential, and C_J is the constant of integration called the Jacobi constant. When the velocity of the particle is zero, $2U = C_J$, a contour represents a zero velocity surface (ZVS) and the motion of a particle within such a surface is considered Hill stable.

γ **Cephei**	**A**	**B**	**Ab**
Mass	1.4 $M_\odot$	0.362 $M_\odot$	1.6 M_J
Semimajor Axis (a)	19.02 AU		1.94 AU
Eccentricity (e)	0.4085		0.115
Argument of Periapsis (ω_p)	0°	180°	94°

Table 1. Orbital parameters of γ Cephei (Neuhauser et. al. 2007)

Gliese 86	**A**	**B**	**Ab**
Mass	0.79 $M_\odot$	0.55 $M_\odot$	3.91 M_J
Semimajor Axis (a)	18.42 AU		0.113 AU
Eccentricity (e)	0.3974		0.0416
Argument of Periapsis (ω_p)	0°	180°	269°

Table 2. Orbital parameters of Gliese 86 (Lagrange et al. 2006; Butler et al. 2006; Santos et al. 2004)

HD 196885	**A**	**B**	**Ab**
Mass	1.33 $M_\odot$	0.45 $M_\odot$	2.98 M_J
Semimajor Axis (a)	21 AU		2.6 AU
Eccentricity (e)	0.42		0.48
Argument of Periapsis (ω_p)	0°	180°	93.2°

Table 3. Orbital parameters of HD 196885, (Chauvin et al. 2007)

HD 41004	**B**	**Ab**	**Bb**
Mass	0.4 $M_\odot$	2.3 M_J	18.64 M_J
Semimajor Axis (a)	22 AU	1.31 AU	0.0177 AU
Eccentricity (e)	0.065	0.39	0.081
Argument of Periapsis (ω_p)	180°	97°	178.5°

Table 4. Orbital parameters of HD 41004, $M_A = 0.7 M_\odot$ (Zucker et al. 2004; Butler et al. 2006)

The measure of Hill stability, $S(f)$, is given by a parameter dependent potential, $\Omega(\mathbf{x}, f)$, where f is the true anomaly and C_{cr} is the value of the Jacobi constant at the Hill radius or the Lagrange point L1 (Szenkovits & Makó 2008)

$$\Omega(x, y, z, f) = \frac{1}{2}\left[x^2 + y^2 - ez^2\cos(f)\right] + \frac{1-\mu}{r_1^2} + \frac{\mu}{r_2^2} + \frac{1}{2}\mu(1-\mu),$$

$$S(f) = \frac{1}{C_{cr}}\left[2\Omega(\mathbf{x}, f) - \left[1 + e\cos(f)\right]v^2\right] - 1. \quad (7)$$

Using the orbital parameters obtained from the numerical integration the potential, $\Omega(\mathbf{x}, f)$, is calculated to obtain the Hill stability function $S(f)$. Although the Hill stability function depends on the true anomaly, it can also be represented as a time series. We have implemented this representation in our results concerning the Hill stability function. When the measure of $S(f)$ of a planet is positive then we

have the indication of quasi-periodic orbits and its motion is Hill stable. But when the measure of $S(f)$ is negative then the planet enters the chaotic region, hence loosing its stability.

2.4 The MEGNO Chaos Indicator

The MEGNO criterion was first introduced by Cincotta & Simó (1999, 2000); Cincotta et al. (2003) and found widespread applications in dynamical astronomy (Goździewski et al. 2001, 2008; Goździewski & Migaszewski 2009; Hinse et al. 2008, 2010; Frouard et al. 2011; Compère et al. 2012; Kostov et al. 2012). The MEGNO (usually denoted as $\langle Y \rangle$) formalism has the following mathematical properties. In general, MEGNO has the parameterisation $\langle Y \rangle = \alpha \times t + \beta$ (see references above). For a quasi-periodic initial condition, we have $\alpha \simeq 0.0$ and $\beta \simeq 2.0$ (or $\langle Y \rangle \to 2.0$) for $t \to \infty$ asymptotically. If the orbit is chaotic, then $\langle Y \rangle \to \lambda t/2$ for $t \to \infty$. Here λ is the maximum Lyapunov exponent (MLE) of the orbit. In practice, when generating our MEGNO maps, we terminate a given numerical integration of a chaotic orbit when $\langle Y \rangle > 12.0$. Quasi-periodic orbits have $|\langle Y \rangle - 2.0| = 0.001$.

We used the MECHANIC[3] software (Słonina et al. 2012) to calculate the MEGNO maps on a multi-CPU computing environment. Typically we allocated 60 CPUs for the calculation of one map considering a typical grid of (500×300) initial conditions in (a, e) space. The numerical integration of the equations of motion and the associated variational equations (Mikkola & Innanen 1999) are based on the ODEX integration software (Hairer et al. 1993) which implements a Gragg-Bulirsch-Stoer algorithm. The MEGNO indicator is calculated from solving two additional differential equations as outlined in Goździewski et al. (2001).

MEGNO and the maximum Lyapunov exponent (MLE) have a close relation and provide the magnitude of the exponential divergence of orbits. Froeschlé et al. (1997) introduced the fast Lyapunov indicator (FLI), which exhibits the least dependency on initial conditions. Recently, Mestre et al. (2011) showed that MEGNO and FLI are related to each other. FLI is used to detect weak chaos and is considered a faster means to determine the same characteristics as MLE. Very recently, Maffione et al. (2011) compared various chaos indicators including FLI and MEGNO. The MEGNO technique and FLI are considered to be in the same class of chaos detection tools (Morbidelli 2002), and we have chosen the MEGNO technique to compare it versus the Hill stability criterion. More on mathematical properties of MEGNO and its relationship with the Lyapunov exponents can be found in Hinse et al. (2010).

3 RESULTS AND DISCUSSION

3.1 Numerical Simulation

To establish the Hill stability (HS) criterion and calculate the maximum Lyapunov exponents (MLE), we numerically simulated each of the planets in the stellar binaries using a Yoshida sixth order symplectic and a Gragg-Bulirsch-Stoer integration scheme (Yoshida 1990; Grazier et al. 1996; Hairer et al. 1993). A stepping of ϵ=10^{-4} years/step was used in each case to have a better measure of the precision of the integration scheme. The error in energy was calculated at each step which falls in the range of 10^{-14} to 10^{-10} during the total integration period. Numerical simulations were completed for a million years to calculate the MLE and 10 million years to calculate the HS. MEGNO maps are calculated using 150,000 years per initial condition.

Calculations involving chaos indicators are unaffected by longer simulation time. Thus, the purpose of simulating for 10 million years was to display the evolution of eccentricity and semi-major axis without applying any indicator tools to provide a consistent comparison in order to analyse the orbital behaviour and to establish the full effectiveness of the indicators. The time series plots for two of the selected systems, γ Cephei and HD 196885, are relatively constant with minor oscillations for 10 million years (Fig. 1). In these cases we found that the eccentricity of the giant planets is oscillating with a constant amplitude. For example, Figs. 1a and 1c demonstrate oscillations from 0 to 0.1 and 0.4 to 0.5 in values of eccentricity for γ Cephei and HD 196885, respectively. The amplitude of the oscillation changed with a different choice of initial conditions. As a result, specific choices can minimise the oscillation amplitude and can render the simulation for γ Cephei to be in closer agreement with previous studies by Haghighipour (2006). One such initial condition involved the choice of eccentricity. If $e = 0$ for the planetary orbit initially, we observed that the amplitude of oscillation is minimum and consistent with Haghighipour (2006) while the amplitude increases with larger initial e values.

3.2 MLE: Indicator Analysis

The maximum Lyapunov exponent (MLE) time series for the simulated planets in the stellar binaries are given in Figs. 2 and 3. The MLE is plotted using a logarithmic scale along the y-axis and a linear scale along the time-axis. We obtained six Lyapunov exponents from our simulation among which three are negative and three are positive. We inspected the first three positive LEs and found the rate of change in magnitude of the largest value which is used for our purpose of establishing the stability of a system.

In Figures 2 and 3, we have taken the maximum Lyapunov exponent as the primary indicator of the orbital stability. For a given initial condition, the MLE must quickly drop below a cutoff value (Quarles et al. 2011) and decrease at a constant rate where we can determine it as stable or unstable. The MLE of the planets within each system show that the observed systems are in stable configurations, as expected from the observations. In each case the MLE starts on the order of 10^1 and slowly converges down by orders of 10. The MLE for γ Cephei, Fig. 2a, starts initially on the order of 1 and quickly drops down to -10 on a logarithmic scale. Then it slowly decreases to -13 in a million years. In the case of Gliese 86, Fig. 2b, the MLE decreases very slowly between -10 and -12. Considering this decreasing trend and the nature of Lyapunov exponents, Section 2.2, the results reflect the outcome of orbital stability for the planet. The MLE for the planet in Gliese 86 also oscillates every 0.3 million years which is indicative of a near resonance behaviour.

[3] http://www.git.astri.umk.pl/projects/mechanic

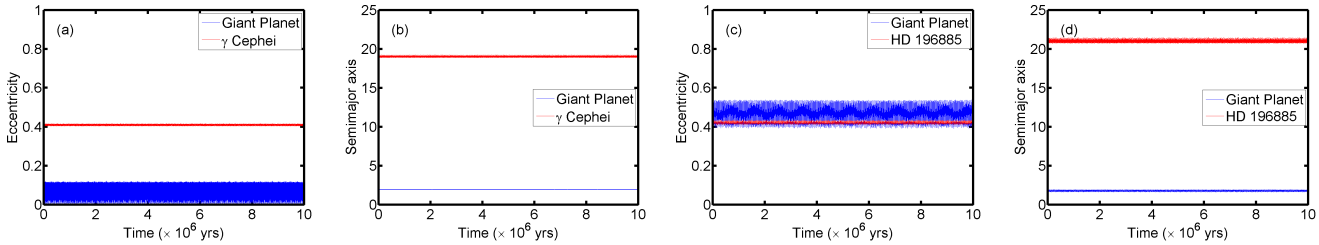

Figure 1. Variation of orbital elements for the giant planet in γ Cephei and HD 196885 simulated for 1×10^7 yrs.

Based on the MLE time series, Fig. 2c, the orbit of the planet in HD 196885 system is in a stable configuration. Similar to the case of γ Cephei, the MLE values for HD 196885 are scattered below its major trend line of -13 displaying the possible perturbation caused by the secondary star. The oscillations observed every 0.2 million years are due to the near resonance behaviour, a similar characteristic shown by the planet in Gliese 86.

Because HD 41004 is a four body system, we examined it in two ways. First, we considered the system setup as an elliptic restricted four body problem with the primary star (A), secondary star (B) and two planets (Ab and Bb) orbiting each of the stars. Then, we separately generated the MLE for each of the planets (Figs. 3a and 3b). We found that for both of the planets, the MLE rapidly decreases until -10 (on a logarithmic scale) and then levels off. The orbital stability is ensured for both of the planets. Secondly, we reduced the system to an elliptic restricted three body problem (ERTBP) to simplify the problem. Since the planet Bb is a brown dwarf, we moved the reduced mass of the planet and its host star to their respective barycentre. Then, with star A and star (B+Bb) in the system we calculated the orbital perturbation on the planet Ab due to the star-planet system (B+Bb). The MLE of the planet Ab, Fig. 3c, is slowly decreasing from -10 to -14, as we would expect. There is not a significant change in the MLE time series of the planet Ab when comparing between the 4 body and 3 body representations; however, the MLE for the reduced system oscillates. In any case the MLE time series indicates stable orbits for the planets in HD 41004 binary system. The reduction allowed us to compare MLE time series for two different models and to generate the MEGNO maps more easily, and was the chosen setup for further analysis in Sect. 3.4.

3.3 Establishing the Hill Stability criterion

The Hill stability time series for the planets in γ Cephei, Gliese 86, HD 196885 and HD 41004 are shown in the Figs. 4 and 5. For all the cases we have considered the stars and the planets to be coplanar ($i = 0^o$).

We found that the measure of Hill stability for γ Cephei stays positive throughout the integration period (10 million years). At intervals of 2-3 and 7-8 million years a spike in the Hill stability is noted, which indicates that the planet shows a quasi-periodic motion every 5 million years. The oscillations on average are small and positive which reflect the condition for HS criteria established by Szenkovits & Makó (2008). Their calculation of Hill stability is positive and constantly increasing in time for a million years, which is consistent with our result. However, the plots are limited to a million years in the calculations of Szenkovits & Makó (2008) which makes the periodicity for long term oscillations for the planets to remain unclear.

Similarly, the Hill stability time series stays positive and constant for the planet in the HD 196885 and Gliese 86 binary systems (Figs. 4b and 4c). The planet in HD 196885 displays a quasi periodic motion every 2 million years. For the planet in Gliese 86, the value of HS initially increases from 0 to 2 million years and then oscillates every 0.3 million years with constant amplitude. The increment of HS value is consistent with Szenkovits & Makó (2008) for the first million years.

At first the values of Hill stability for the planets in the HD 41004 binary system was calculated by considering the system as an elliptic restricted four body problem. The Hill stability time series of the planets are shown in Figs. 5a and 5b. The HS values for the planets in HD 41004 Ab and Bb are oscillating with an amplitude ranging from 0-200 and 0-100 respectively. Since the stability function S(f) remains positive for the entire simulation time, we can conclude that the system is Hill stable. The Hill stability function calculated by Szenkovits & Makó (2008) for the same planets is positive but constantly increasing for HD 41004 Ab and constantly decreasing for HD 41004 Bb. In our results the stability values are increasing for the first half million years and remain constant thereafter. Szenkovits & Makó calculated the HS for only a million years and our HD 41004 Ab result is consistent with their previous study. However, for HD 41004 Bb, the positive HS values are constantly decreasing which indicates that the planet my loose its stability beyond one million years.

The HS time series for HD 41004 system indicates orbital stability of the planets Ab and Bb due to the fact that the HS values remain positive. However, the HS values for both the planets are noisy and randomly fluctuating because it was represented as a four body system. This might be due to the small perturbations caused by the brown dwarf Bb which has the mass of 18.64 M_j (Tab. 4) and considering that the Hill stability function is not general enough to describe this particular system. Thus it is important to note that the establishment of stability using this method will be restricted to three body systems. Since significant results from this calculation were not produced, we stopped the simulation at 8 million years. Thus we became motivated to modify the HD 41004 system into an ERTBP (Sect 3.2) and measured the HS values for the planet Ab, shown in Fig. 5c. The HS value is constant, positive and demon-

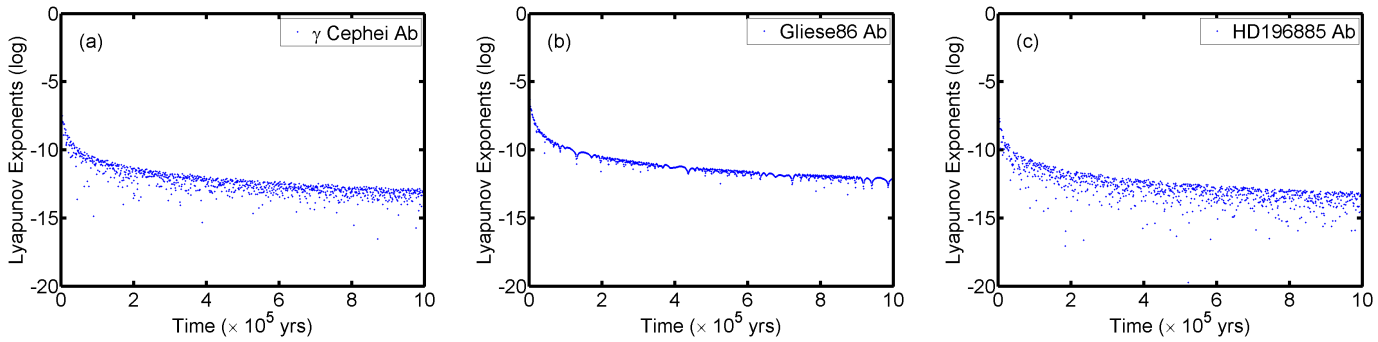

Figure 2. Variation of Lyapunov time series for the giant planet in (a) γ Cephei, (b) Gliese 86 and (c) HD 196885 simulated for 1×10^6 years.

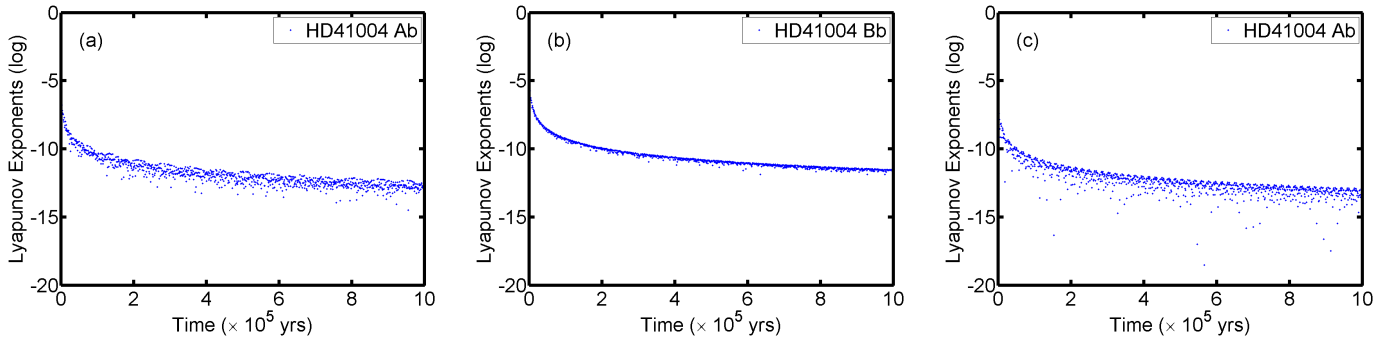

Figure 3. Variation of Lyapunov time series for the giant planet as a 4 body problem in (a) HD 41004 Ab and (b) HD 41004 Bb. Variation of Lyapunov time series for the giant planet Ab as a 3 body problem (c). Each figure was simulated for 1×10^6 years.

strates quasi-periodic oscillations every three million years. The amplitude of oscillations reaches a maximum every six million years.

The planet in the HD 41004 system displayed a positive stability for the coplanar case irrespective of our choice of model.

3.4 Analysis of MEGNO maps

The MEGNO indicators are generated over a 150,000 initial conditions in eccentricities and semi-major axes for the respective planets within the selected binaries. In Figs. 6, 7, 8 and 9 MEGNO maps for different binary eccentricity were simulated for 100,000 years. The cross hair in each subplot represents the osculating orbit of planet Ab for the respective binary (see tables 1 to 4). The colour bar on top of each map indicates the strength in the value of MEGNO($< Y >$). The blue colour denotes regions of quasi-periodicity and the yellow indicates regions of chaos.

For different eccentricity values of the binary in γ Cephei, Fig. 6, the MEGNO indicator shows a clear distinction between quasi-periodic and chaotic regions. Within the observational value, $e_{bin} = 0.4085$ (Fig. 6a), the planet unmistakably demonstrates stable orbits. When the binary eccentricity, e_{bin}=0.2 (Fig. 6b), is decreased the cross hair is completely inside the quasi-periodic region, hence increasing the orbital stability. Conversely, as the eccentricity of the binary orbit is increased the location of the chaotic mean-motion resonances (yellow spikes at constant semi-major axis) are shiftet to lower semi-major axis of the planet (Fig. 6c).

Figure 7a shows a stable region for the planet in Gliese 86 system. When the e_{bin} is reduced to 0.2 the quasi periodic region increases (Fig. 7b), indicating that the system gets more stable for less eccentric orbits. In Figs. 7b and c, we have only considered the semi-major axis interval to be [1,4] AU because the observed region [0,1] AU remains unchanged with different choices of eccentricity. As a result this causes the cross hair to disappear and displays a more chaotic region to the right. For a circular binary orbit almost all the (a,e) space is quasi-periodic/regular. This is also true for the inner region where we have the planet. When the e_{bin} is increased to 0.6, the chaotic yellow region grows but without endangering the orbital stability of the observed planet.

Figure 8a shows a locally stable region for the planet in HD 196885 system. The cross hair in the map is located right at the edge of the stable region. A small change in semi-major axis of the planet can divert the planet towards the chaotic region loosing global stability. Quasi-periodicity increases with a decrease in the binary eccentricity, Fig. 8b, while the system becomes chaotic with increment in binary eccentricity, Fig. 8c.

The planet (Ab) in HD 41004 binary system, Fig. 9, has stable orbits even when the binary eccentricity varies

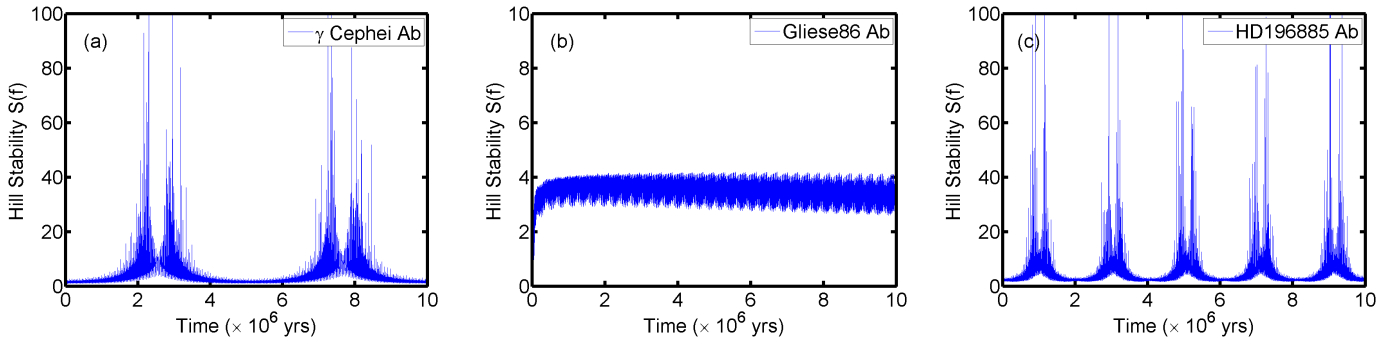

Figure 4. Variation of Hill Stability for the giant planet in (a) γ Cephei, (b) Gliese 86 and (c) HD 196885 simulated for 1×10^7 yrs.

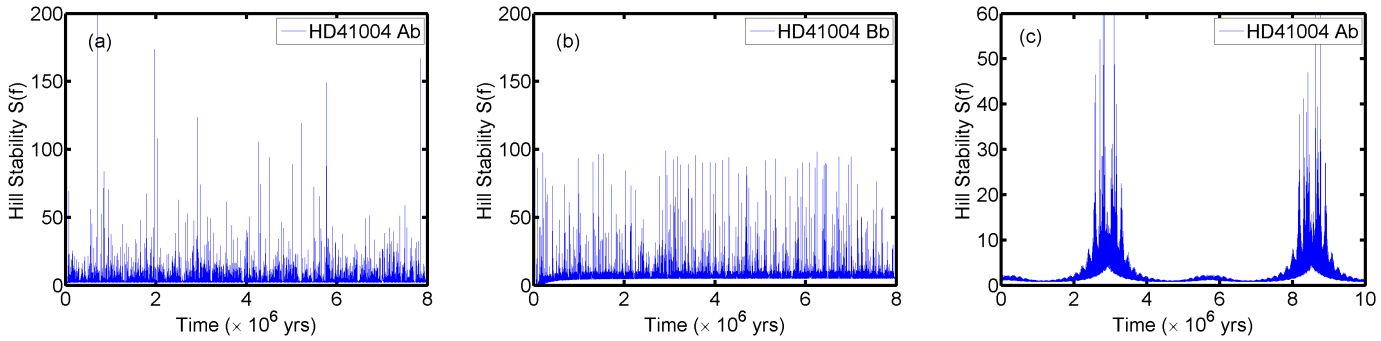

Figure 5. Variation of Hill Stability for the giant planets in HD 41004 as 4 body system (a) and (b), and modified 3 body system (c) simulated for 1×10^7 yrs.

from 0 to 0.6. Although the planet has a relatively high eccentricity (0.39), it resides within the quasi-periodic region and maintains global stability.

3.5 Comparison of Indicators

The maximum Lyapunov exponent for the planet in γ Cephei demonstrates stable orbits. The positive value and non-decreasing global trend of Hill stability time series provides the necessary evidence. The HS times series also indicates that the system is quasi-periodic every 5 million years. Since the calculation for MLE is limited to 1 million years, we are unable to notice any periodicity in the spectra as seen in the HS time series but it does also indicate trends toward stability. The cross hair in Fig. 6a lies in the quasi periodic region of the MEGNO map. Thus, γ Cephei binary system is stable and supplements two of our earlier results.

The MLE time series, Fig. 2b, calculated for the planet in Gliese 86 system shows an oscillating behaviour every 0.3 million years. The HS time series, Fig. 4a, demonstrates a similar oscillation pattern and confirms the comparability of the two indicators. The cross hair seen at the periodic region of MEGNO map (Fig. 7a) again confirms the stability; however, no direct information could be extracted regarding the oscillation.

The MLE, HS time series, and the MEGNO map for the planet in HD 196885 system indicate stable orbits, Figs. 2c, 4c, 8a respectively. The HS spectra is quasi-periodic and oscillates every 2 million years. This cannot be deduced from the MLE spectra. The MEGNO map on the other hand displays a quasi-periodic nature right at the nominal value of semi-major axis 2.6 AU.

The constantly decreasing MLE time series, the positive HS time series, and the MEGNO map cross hair is a clear indication of stability of the planet in the modified HD 41004 system (Figs. 3c, 5c, 9a). The time series obtained from the MLE and HS values for 1 million years both display small oscillations. The reduction of the system from 4 body to 3 body problem does not affect our MLE calculations but significantly affects the HS function and MEGNO indicator. The HS values of the planets in the 4 body are noisy and produce unusable results while in the reduced system we obtain the oscillating HS values every 3 million years which demonstrates the quasi-periodicity of the planet. The MEGNO maps for the reduced system indicate the clear stability of the planet.

3.6 Runtime Comparison

Runtime comparison is vital while comparing the efficiency of various indicators due to the fact that timing is crucial part of numerical integration. The CPU time depends on the computing architecture and integration scheme. We used a Yoshida sixth order symplectic integration scheme to calculate the MLE time series and a Gragg-Bulirsch-Stoer integration scheme from Grazier et al. (1996) and Hairer et al.

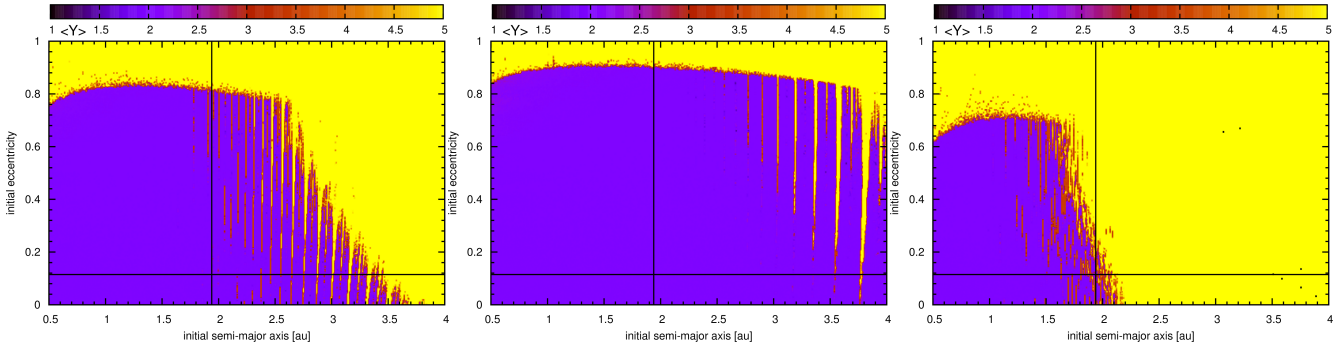

(a) $e_{bin} = 0.4085$ (b) $e_{bin} = 0.2$ (c) $e_{bin} = 0.6$

Figure 6. MEGNO Maps for the planets in γ Cephei simulated for 100,000 years.

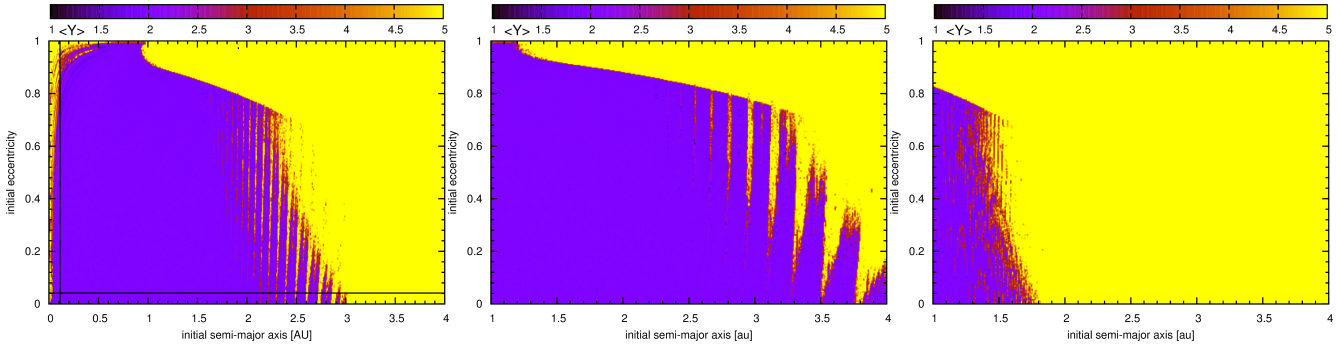

(a) $e_{bin} = 0.3974$ (b) $e_{bin} = 0.2$ (c) $e_{bin} = 0.6$

Figure 7. MEGNO Maps for the planets in Gliese 86 simulated for 100,000 years.

Runtime	MLE	MEGNO	Hill Stability
1000 years	00:13:27	00:00:01	00:03:55
10,000 years	02:16:15	00:00:04	00:35:30
1,000,000 years	$\sim$ 22 Days	00:05:25	$\sim$ 3.5 Days

Table 5. Runtime comparison for different chaos indicators in time format of HH:MM:SS. The MLE, MEGNO and HS are computed for one initial condition for γ Cephei (Table 1) over given period of time and the net CPU run times are compared.

(1993) to calculate the HS time series and MEGNO maps respectively. We believe that one of the reasons for the runtime variation is due to the different implementations of the Gragg-Bulirsch-Stoer integration scheme. Our runtime comparison is made for γ Cephei with the nominal initial conditions given in Table 1. The CPU time to execute each of the indicators (MLE, HS time series and MEGNO maps) for three different time periods are displayed in Table 5. An extensive comparison of runtime is beyond the scope of this paper and subject to future studies.

The Maximum Lyapunov exponent and the Hill stability time series were calculated using Intel(R) Xenon(R) CPU E5345 @ 2.33GHz and the MEGNO maps were generated using a similar computing architecture, Intel(R) CPU(X5355) @ 2.66GHz. The CPU run times shown in Table 5 indicates that it requires longest amount of time to generate MLE time series. The HS time series takes the modest time. MEGNO happens to be the fastest to calculate compared to two others for a given initial condition (IC). The results discussed in this paper were obtained by using one IC for MLE and HS time series and 150,000 ICs for MEGNO maps. For what we want to achieve from the HS time series, single IC would suffice which could be obtained in relatively short amount of time.

3.7 Implications on Habitability

Based on our previous discussion we know that each planet in the four binary stellar systems, γ Cephei, Gliese 86, HD 196885 and HD 41004 exists within a stable orbital configuration. Therefore, the existence of other Earth-like planets in these systems is a plausible assumption. Most of these binary systems have only one planet detected around the primary star. Our stability calculations using the MEGNO indicator shows a probable region where other possible planets could exist.

For the planet (Ab) in γ Cephei, eccentricity-semimajor axes cross hair lies at [0.115, 1.94] AU. The habitable zone (HZ) of the primary star is approximately between [3.05-3.7] AU (Haghighipour 2006). The quasi-periodic regions in the MEGNO map, Fig. 6a, clearly shows some stability islands between [3.0-3.5] AU. For other binary systems, Gliese 86, HD 196885 and HD 41004, the HZ is approximated between [0.018-1.214] AU, [1.333-2.660] AU and [0.762-1.497] AU, respectively (Jones et al. 2006). Our MEGNO maps for Gliese

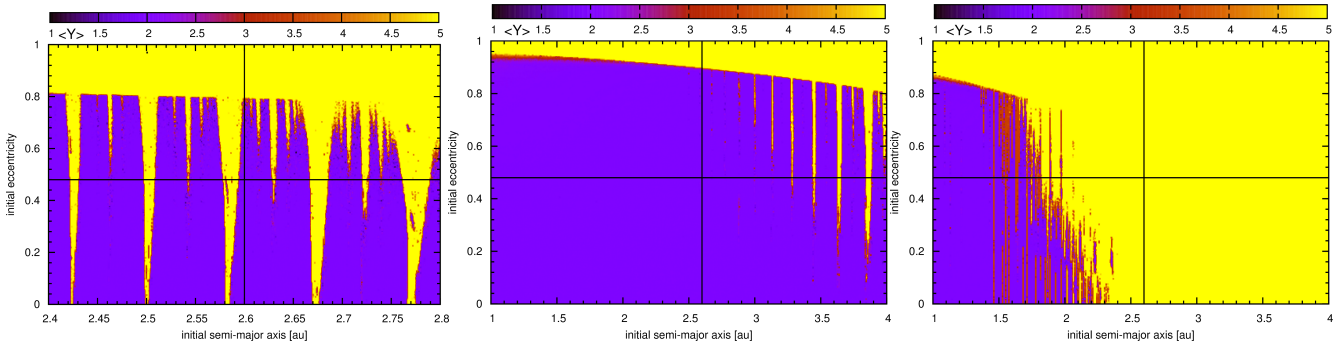

(a) $e_{bin} = 0.42$ (b) $e_{bin} = 0.2$ (c) $e_{bin} = 0.6$

Figure 8. MEGNO Maps for the planets in HD 196885 simulated for 100,000 years.

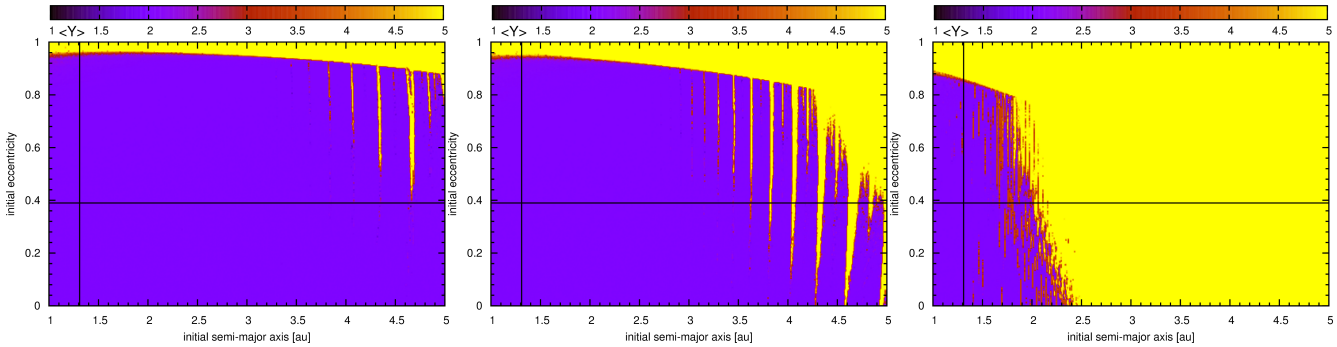

(a) $e_{bin} = 0.065$ (b) $e_{bin} = 0.2$ (c) $e_{bin} = 0.6$

Figure 9. MEGNO Maps for the planets in HD 41004 simulated for 100,000 years.

86 and HD 41004 (Figs. 7a and 9a) display a continuous HZ well inside the limits mentioned above. The MEGNO map for HD 196885 (Fig. 8a) also displays stability islands within the HZ. An Earth-mass test particle can be placed in this region and checked for the stability of the system, and eventually looking for the planets in the continuous habitable zone.

4 CONCLUSIONS

We have applied various chaos indicator techniques in order to study the stability of S-type planets in the binaries that are less than 25 AU apart. With the time series obtained from the maximum Lyapunov exponent and the Hill stability function and the maps from the MEGNO indicator, we have shown that all the systems are in a stable configuration.

Our MLE times series for all four planets converge exponentially which resembles stable planetary orbits. With the MLE oscillating every 0.3/0.2 million years in the case of Gliese 86 Ab/HD 196885 Ab could be indicative of the near resonance behaviour. Similar behaviour is observed in the MLE time series of HD 41004 Ab when reduced to 3 body problem. Our quest of stability analysis using the MLE time series is unaffected by choice of different models of the binary system, HD 41004.

The MEGNO chaos indicator has been effective in determining the quasi-periodic regions. The location of eccentricity-semimajor axis cross hairs in the MEGNO maps for the planets in Gliese 86 and HD 41004 (3 body) systems (Figs. 7a and 9a) are well inside the blue region which resembles the global stability of the planets. The orbital stability of these planets are also unaffected by the highly eccentric ($e_{bin} = 0.6$) binary orbits. For the γ Cephei and HD 196885 systems (Figs. 6a and 6b), the cross hairs are located in the teeth between the chaotic and quasi periodic regions. This resembles the local stability of the planets. These planets do not survive if the binary orbits are highly eccentric.

The chaotic and quasi periodic regions observed in the eccentricity vs. semi-major axis grid of MEGNO maps were the advantage over our two indicators, MLE and HS time series, and we used it to explain the possible existence of planets in the habitable zone. Each of our chosen binary systems shows a possibility of a planet residing within the respective habitable zone.

The Hill stability time series for a planet is successfully measured using the potential obtained from numerical integration of orbital parameters in elliptic restricted three body problem. The measure of the Hill stability is highest at 2.5 million years and 3 million years for the case of γ Cephei, and this feature is observed to repeat every 5 million years. The HS values, nevertheless, stay positive. Similar is the case for HD 196885 and HD 41004 (3 body) systems where the maximum HS is measured every 2 million years and 3 million years respectively. The HS values for the planet in Gliese 86 system first rises up to 4 and changes very little in time. This planet is less perturbed by the secondary star.

The analysis of MEGNO indicator for Gliese 86 Ab shows a similar results where the planet demonstrates global stability. These stability values, for any given system, can be extrapolated beyond our 10 million years integration time and the stability criteria would still hold true. The HS values of γ Cephei Ab, Gliese 86 Ab, and HD 41004 Ab agree with the calculations made by Szenkovits & Makó (2008) when the orbital inclination is zero for each system.

We are able to successfully test the efficacy of Hill stability against LEs and MEGNO chaos indicators. Direct comparison of stability shows that the Hill stability can be set as one of three stringent criterion in the study of stable/unstable nature of an planetary orbit in the ERTBP. Numerical simulations for the HS function is faster than the MLE but slower than the MEGNO indicator. Our results show that the HS indicator is comparable to the other indicators and through our qualitative efficiency analysis we have demonstrated that HS can be used as an alternative to MLE.

Acknowledgement: SS and BQ would like to thank department of Physics UT Arlington, Zdzislaw Musielak and Manfred Cuntz for their continuous support and guidance. TCH gratefully acknowledges financial support from the Korea Research Council for Fundamental Science and Technology (KRCF) through the Young Research Scientist Fellowship Program and financial support from KASI (Korea Astronomy and Space Science Institute) grant number 2012-1-410-02. Numerical computations were partly carried out using the SFI/HEA Irish Centre for High-End Computing (ICHEC) and the PLUTO computing cluster at the Korea Astronomy and Space Science Institute. Astronomical research at the Armagh Observatory is funded by the Northern Ireland Department of Culture, Arts and Leisure (DCAL).

REFERENCES

Benettin G., Galgani L., Giorgilli A., Strelcyn J.-M., 1980, Meccanica, 15, 9

Borucki W., Koch D., Basri G., Batalha N., Brown T., Caldwell D., Christensen-Dalsgaard J., Cochran W., Dunham E., Gautier T. N., Geary J., Gilliland R., Jenkins J., Kondo Y., Latham D., Lissauer J. J., Monet D., 2008, in Sun Y.-S., Ferraz-Mello S., Zhou J.-L., eds, IAU Symposium Vol. 249 of IAU Symposium, Finding Earth-size planets in the habitable zone: the Kepler Mission. pp 17–24

Borucki W. J., Koch D., Basri G., Batalha N., Brown T., Caldwell D., 2010, Science, 327, 977

Borucki W. J., Koch D. G., Dunham E. W., Jenkins J. M., 1997, in Soderblom D., ed., Planets Beyond the Solar System and the Next Generation of Space Missions Vol. 119 of Astronomical Society of the Pacific Conference Series, The Kepler Mission: A Mission To Detennine The Frequency Of Inner Planets Near The Habitable Zone For A Wide Range Of Stars. p. 153

Butler R. P., Wright J. T., Marcy G. W., Fischer D. A., Vogt S. S., Tinney C. G., Jones H. R. A., Carter B. D., Johnson J. A., McCarthy C., Penny A. J., 2006, *ApJ* , 646, 505

Chauvin G., Lagrange A.-M., Udry S., Mayor M., 2007, *A&A* , 475, 723

Cincotta P., Simó C., 1999, Celestial Mechanics and Dynamical Astronomy, 73, 195

Cincotta P. M., Giordano C. M., Simó C., 2003, Physica D Nonlinear Phenomena, 182, 151

Cincotta P. M., Simó C., 2000, aaps, 147, 205

Compère A., Lemaître A., Delsate N., 2012, Celestial Mechanics and Dynamical Astronomy, 112, 75

Desidera S., Barbieri M., 2007, *A&A* , 462, 345

Duquennoy A., Mayor M., 1991, *A&A* , 248, 485

Froeschlé C., Lega E., Gonczi R., 1997, Celestial Mechanics and Dynamical Astronomy, 67, 41

Frouard J., Vienne A., Fouchard M., 2011, *A&A* , 532, A44

Gonczi R., Froeschle C., 1981, Celestial Mechanics, 25, 271

Goździewski K., Bois E., Maciejewski A. J., Kiseleva-Eggleton L., 2001, *A&A* , 378, 569

Goździewski K., Breiter S., Borczyk W., 2008, mnras, 383, 989

Goździewski K., Maciejewski A. J., 2001, *ApJL* , 563, L81

Goździewski K., Migaszewski C., 2009, *MNRAS* , 397, L16

Grazier K. R., Newman W. I., Varadi F., Goldstein D. J., Kaula W. M., 1996, in AAS/Division of Dynamical Astronomy Meeting #27 Vol. 28 of Bulletin of the American Astronomical Society, Integrators for Long-Term Solar System Dynamical Simulations. p. 1181

Haghighipour N., 2006, *ApJ* , 644, 543

Hairer E., Norsett S. P., Wanner G., 1993, Solving Ordinary Differential Equations I, nonstiff problems, 2nd Ed., Springer Series in Computational Mathematics (Springer-Verlag)

Hilborn R. C., Sprott J. C., 1994, American Journal of Physics, 62, 861

Hill G. W., 1878a, *MNRAS* , 38, 192

Hill G. W., 1878b, Astronomische Nachrichten, 91, 251

Hinse T. C., Christou A. A., Alvarellos J. L. A., Goździewski K., 2010, *MNRAS* , 404, 837

Hinse T. C., Michelsen R., Jørgensen U. G., Goździewski K., Mikkola S., 2008, *A&A* , 488, 1133

Jones B. W., Sleep P. N., Underwood D. R., 2006, *ApJ* , 649, 1010

Koch D., Borucki W., Basri G., Brown T., Caldwell D., Christensen-Dalsgaard J., Cochran W., Devore E., Dunham E., Gautier T. N., Geary J., Gilliland R., Gould A., Jenkins J., Kondo Y., Latham D., Lissauer J., Monet D., 2007, in Hartkopf W. I., Guinan E. F., Harmanec P., eds, IAU Symposium Vol. 240 of IAU Symposium, The Kepler Mission and Eclipsing Binaries. pp 236–243

Kostov V. B., McCullough P., Hinse T., Tsvetanov Z., Hébrard G., Díaz R., Deleuil M., Valenti J. A., 2012, ArXiv e-prints

Lagrange A.-M., Beust H., Udry S., Chauvin G., Mayor M., 2006, *A&A* , 459, 955

Lyapunov A., 1907, Annales de la facultè des sciences de Toulouse, 2:9, 203

Maffione N. P., Darriba L. A., Cincotta P. M., Giordano C. M., 2011, Celestial Mechanics and Dynamical Astronomy, 111, 285

Marchal C., Bozis G., 1982, Celestial Mechanics, 26, 311

Mayor M., Queloz D., 1995, *Nature* , 378, 355

Mestre M. F., Cincotta P. M., Giordano C. M., 2011, *MNRAS* , 414, L100

Mikkola S., Innanen K., 1999, Celestial Mechanics and Dynamical Astronomy, 74, 59
Morbidelli A., 2002, Modern celestial mechanics : aspects of solar system dynamics
Murray C. D., Dermott S. F., 1999, Solar system dynamics
Murray N., Holman M., 2001, nat, 410, 773
Musielak Z. E., Musielak D. E., 2009, International Journal of Bifurcation and Chaos, 19, 2823
Ott E., 1993, Chaos in dynamical systems
Ozorio de Almeida A. M., 1990, Hamiltonian Systems
Quarles B., Eberle J., Musielak Z. E., Cuntz M., 2011, A&A, 533, A2
Raghavan D., Henry T. J., Mason B. D., Subasavage J. P., Jao W.-C., Beaulieu T. D., Hambly N. C., 2006, *ApJ* , 646, 523
Raghavan D., McAlister H. A., Henry T. J., Latham D. W., Marcy G. W., Mason B. D., Gies D. R., White R. J., ten Brummelaar T. A., 2010, *ApJS* , 190, 1
Santos N. C., Israelian G., Mayor M., 2004, *A&A* , 415, 1153
Słonina M., Goździewski K., Migaszewski C., 2012, in Arenou F., Hestroffer D., eds, Proceedings of the workshop "Orbital Couples: Pas de Deux in the Solar System and the Milky Way". Held at the Observatoire de Paris, 10-12 October 2011. Editors: F. Arenou, D. Hestroffer. ISBN 2-910015-64-5, p. 125-129 Mechanic: a new numerical MPI framework for the dynamical astronomy. pp 125–129
Szebehely V., 1967, Theory of orbits. The restricted problem of three bodies
Szebehely V., 1980, Celestial Mechanics, 22, 7
Szebehely V., McKenzie R., 1981, Celestial Mechanics, 23, 3
Szenkovits F., Makó Z., 2008, Celestial Mechanics and Dynamical Astronomy, 101, 273
Tsonis A., 1992, Chaos: from theory to applications. Plenum Press
Walker I. W., Roy A. E., 1981, Celestial Mechanics, 24, 195
Wolf A., Swift J. B., Swinney H. L., Vastano J. A., 1985, Physica D Nonlinear Phenomena, 16, 285
Yoshida H., 1990, Physics Letters A, 150, 262
Zhou L.-Y., Dvorak R., Sun Y.-S., 2009, *MNRAS* , 398, 1217
Zucker S., Mazeh T., Santos N. C., Udry S., Mayor M., 2004, VizieR Online Data Catalog, 342, 60695